of an intricate balance of the various intramolecular interactions, rather than the results of crystal packing forces.

It is important to know the "active" conformation of thiamin, apart from the "stable" conformation, because it can be directly correlated with the functional property of the 4'-amino group. The present structure along with the high affinity of TT for the apoenzyme suggests that the conformation of the enzyme-bound free thiamin may be the V form. If TT assumes a different conformation upon binding, the intramolecular hydrogen bond has to be broken and it would be energetically unfavorable. Although the most stable conformation of free thiamin seems to be the F form, a conformational change to V may take place upon binding to the apoenzyme. The energy barrier between the different conformers is known to be small as shown by semiempirical energy calculations[33] (less than 6 kcal/mol) and by NMR studies.[6] Therefore, conversion of F or S to V via concerted rotation of the two rings about the methylene bridge can be achieved easily. It is worthwhile to notice that oxythiamin in the V form can also bind to the apoenzyme as strongly as thiamin does although it cannot release the product.[4a]

From the kinetic studies of the binding processes of TTPP to pyruvate decarboxylase, Kruger et al. concluded that the high affinity of TTPP for the apoenzyme is mainly due to its lower polarity and that TTPP resembles an intermediate rather than a transition state.[12] The present study shows that the conformational characteristics of TT, as well as the neutral thiazole moiety, certainly contribute to its low polarity since one of the amino hydrogens is engaged in an intramolecular hydrogen bond. Apart from the question of whether TTPP is a transition-state analogue or not, the present study suggests that the conformational differences do exist between thiamin and TT and thus may affect the binding efficiency. If the active form of free thiamin is the V form, one of the functions of the apoenzyme may be to hold the coenzyme in the V conformation. If this is the case, the 4'-amino group can directly participate in the catalytic process, or at least serve to direct the incoming substrate properly. However, further studies have to be done to know whether the 4'-amino group is directly involved in acid-base catalysis.

Acknowledgment. We thank the referees for the valuable comments. This work was supported by a grant from the Korea Science and Engineering Foundation.

Registry No. Thiamine thiazole, 490-82-4.

Supplementary Material Available: Tables S1-S3 listing anisotropic thermal parameters, coordinates of the hydrogen atoms, and bond distances and angles involving the hydrogen atoms (3 pages); tables of observed and calculated structure factors (10 pages). Ordering information is given on any current masthead page.

(33) Jordan, F. *J. Am. Chem. Soc.* **1974**, *96*, 3623-3630.

NMR Studies of the Binding of Sodium and Calcium Ions to the Bile Salts Glycocholate and Taurocholate in Dilute Solution, as Probed by the Paramagnetic Lanthanide Dysprosium

Elizabeth Mukidjam,[†] Stephen Barnes,[†‡⊥] and Gabriel A. Elgavish*[‡§]

Contribution from the Departments of Pharmacology and Biochemistry, Cardiac NMR Laboratory, Division of Cardiovascular Disease, and The Comprehensive Cancer Center, University of Alabama at Birmingham, Birmingham, Alabama 35294.
Received February 21, 1986

Abstract: The role of calcium in the biliary and intestinal milieu may be quite central, forming physiologically important complexes of bile salts. The binding of Ca^{2+} to bile salts in aqueous solution, in particular to glycocholate and taurocholate, has been investigated by using Ca^{2+}-specific electrodes. The reported dissociation constants are surprising since they suggest that the sulfonate-bearing taurocholate has a greater affinity for Ca^{2+} than the carboxylate-bearing glycocholate. Hydroxyl involvement in Ca^{2+} binding to glycocholate has also been suggested (Moore, E. *Hepatology* **1984**, *4*, 228S-243S). This may bring geometrical contraints on the molecule, which may result in a thermodynamic preference for binding in the case of taurocholate vs. that in the glycocholate system. In the present study we have used a paramagnetic NMR approach in which the lanthanide ion Dy^{3+}, an isomorphous replacement for Ca^{2+}, causes concentration-dependent stereospecific changes in the bile salt ^1H chemical shifts. The dysprosium-induced effects have been modulated by the addition of $CaCl_2$ or NaCl. Analysis of the data by nonlinear computer programs has enabled calculation of the metal-bile salt dissociation constants for Dy^{3+}, Ca^{2+}, and Na^+ complexes. For each metal ion the dissociation constant of the metal-bile salt complex was 2-6 times larger for taurocholate than for glycocholate. These data are consistent with the idea that the Ca^{2+} ion has a greater affinity for the carboxylate group than for the sulfonate group. The intrinsic shifts of ^1H resonances, which are sensitive to changes in the position of the Dy^{3+} ion, decrease gradually for protons the further they are from the carboxylate end, indicating metal binding to the carboxylate group. These intrinsic shifts are unaltered in the presence of $CaCl_2$ or NaCl, suggesting that Ca^{2+} competes for binding to the anionic group and not to any other site on the bile salt molecule.

Bile salts are the most important natural detergents. They have amphiphilic properties and in aqueous solution, above their critical micellar concentration, undergo self-association, forming micellar complexes.[1,37] In bile they form mixed micellar aggregates with phospholipids and cholesterol,[2] while in the small intestines micellar aggregates of bile salts with fatty acids and glycerides occur.[3] These micellar species have a multifaceted role in the gastrointestinal system. They disperse triglycerides, enhance the activity of lipases, and solubilize fatty acids and monoglycerides, the

[†] Department of Pharmacology.
[‡] Department of Biochemistry.
[§] Division of Cardiovascular Disease.
[⊥] The Comprehensive Cancer Center.

(1) Small, D. M. In *The Bile Acids, Chemistry, Physiology and Metabolism*; Nair, P. P., Kritchevsky, D., Eds.; Plenum: New York, 1971; Vol. I, pp 249-356.
(2) Carey, M. C.; Small, D. M. *J. Clin. Invest.* **1978**, *61*, 998-1026.
(3) Hofmann, A. F. *Biochem. J.* **1963**, *89*, 57-68.

0002-7863/86/1508-7082$01.50/0

products of lipase activity.[4] Bile salt micelles are also thought to be the vehicles for the transport of lipid-soluble substances, e.g., vitamin D,[5] in the aqueous milieu of the intestinal lumen. Metal cations, in particular Ca^{2+}, have been implicated as having a role in these different functions of bile salts. The natural bile salts all have negatively charged functional groups, as well as polar hydroxy groups, for their interaction with metal ions.

Interaction of bile salts with polyvalent metal ions, such as Ca^{2+}, forming soluble complexes of moderate stability, has a possible role in the function of bile salts. Formation of Ca^{2+}–bile salt complexes may also serve as a mechanism to buffer free Ca^{2+} activity in the gastrointestinal system. Indeed, recent investigations[6-10] have shown that a significant fraction of Ca^{2+} in the bile is bound to bile salts. One of the results of Ca^{2+}–bile salt interaction may be a lowered probability of the precipitation of insoluble calcium salts.

Prevention of calcium precipitation by complexation with bile salts has attracted attention since it has provided insight into the cause of cholesterol and pigment gallstone formation. Such gallstones often contain centers consisting of precipitated calcium salts. Reduction of the Ca^{2+} activity in bile may be an important factor in the prevention of gallstone formation.[11]

Currently, two bile salts, 3α,7α-dihydroxy-5β-cholan-24-oate (chenodeoxycholate) and 3α,7β-dihydroxy-5β-cholan-24-oate (ursodeoxycholate), are in clinical use for the dissolution of cholesterol-rich gallstones.[12,13] Some difficulties have been encountered with ursodeoxycholate due to calcium-rich regions in the stone.[14] However, this is not thought to be caused by poor complexation of Ca^{2+} by ursodeoxycholate. In fact, the latter binds Ca^{2+} more effectively than other bile acids.[15] Rather, the effect is due to stimulation of biliary bicarbonate secretion by ursodeoxycholate.[11,16]

The complexation of Ca^{2+} by bile salts has been recently investigated by using Ca^{2+}-specific electrodes. Dissociation constants of 6.6 mM for monomeric complexes of Ca^{2+}–taurocholate and 13.3 mM for Ca^{2+}–glycocholate have been reported.[17] At bile salt concentrations typical of micellar solutions, dissociation constants of 140 and 161 mM were found for the Ca^{2+}–taurocholate and the Ca^{2+}–glycocholate complexes, respectively. These results have indicated a somewhat higher Ca^{2+} binding affinity of taurocholate relative to that of glycocholate.

Contrary to these results, the carboxylate group is known to have higher affinity for Ca^{2+} and for other non-transition-metal ions than other anionic groups.[18] Consequently, one would expect a lower dissociation constant for Ca^{2+} complexed to the carboxylate-bearing glycocholate than for Ca^{2+} bound to the sulfonate group of taurocholate. On the other hand, hydroxy groups of the cholanoate moiety may also be involved in Ca^{2+}–bile salt binding. In that case, the longer, therefore more flexible, taurocholate side chain may more easily accommodate simultaneous side-chain and hydroxy binding. This may increase binding affinity relative to that in the glycocholate system. Indeed, involvement in calcium binding to the hydroxys, in particular the hydroxy in the 7-position, has been suggested.[19]

In the present work, we set out to study Ca^{2+} binding to glycocholate and taurocholate by a technique that meets several requirements. (i) Binding is monitored by virtue of a direct perturbation of an observable physical property of the bile salt that results from metal-ion binding, rather than by monitoring the complexation-effected reduction in the concentration of free Ca^{2+}, which is the essence of most techniques, e.g., the method of monitoring complexation by the Ca^{2+}-specific electrode. (ii) Measurements can be done in a concentration range close to the magnitude of the dissociation constants of the complexes involved.[20,21] (iii) The observable perturbation caused by the metal-ion binding should be stereospecific, so that the binding site, or sites if more than one is possible, can be determined. These requirements are absolutely necessary to enable answers to the outstanding questions of the Ca^{2+}–bile salt systems.

The studies presented here have been carried out by analysis of lanthanide-induced paramagnetic nuclear magnetic resonance (NMR) effects. The technique of choice is the monitoring of the paramagnetic perturbations induced in the ^1H NMR resonances of glycocholate and taurocholate by the binding of the lanthanide ion Dy^{3+}. The lanthanides, 4f transition metals with largely non-transition-metal-like chemistry, are considered as isomorphous replacements for calcium.[22-27] Unlike Ca^{2+}, however, lanthanide ions display a range of useful spectroscopical properties. Therefore, they have been widely used to determine stoichiometries and affinities of Ca^{2+}-binding sites on proteins and other biologically important molecules.[24,28] The NMR chemical shift changes, induced by the binding of the paramagnetic lanthanide ion, are a property of the bile salt molecule in its metal-bound state only. Therefore, the measured effect is directly proportional to the equilibrium concentration of the complex. The NMR measurements can be carried out conveniently at the millimolar-to-tens of millimolar range of concentration of the components of the solution, offering a close to optimal range corresponding to the determined dissociation constants. Furthermore, since the dipolar, paramagnetic interaction between the lanthanide ion and the nuclei of the various hydrogen atoms in the bile salt molecule is strongly dependent on the distance between a given nucleus and the metal ion, as well as on the angular position, the metal-binding sites can be identified. Thus, paramagnetic NMR is the method of choice to delineate binding in these complex systems.

We have carried out binding experiments by NMR on the Dy^{3+}–glycocholate and Dy^{3+}–taurocholate complexes and determined their dissociation constants and stoichiometries. The dissociation constants of the calcium complexes and the sodium complexes of these two bile salts have been determined by monitoring the quantitative effects of the competition of Ca^{2+} and Na^+ ions on the binding of the Dy^{3+} ion. For the Ca^{2+} and Dy^{3+} ions,

(4) Carey, M. C. In *The Liver: Biology and Pathobiology*; Arias, I., Popper, H., Schachter, D., Shafritz, D. A., Eds.; Raven: New York, 1982; pp 429–465.
(5) Norman, A. W. *Vitamin D. Molecular Biology and Clinical Nutrition*; Marcel Dekker: New York, 1979; p 533.
(6) Williamson, B. W. A.; Percy-Robb, I. W. *Biochem. J.* **1979**, *181*, 61–66.
(7) Williamson, B. W. A.; Percy-Robb, I. W. *Gastroenterology* **1980**, *78*, 696–702.
(8) Rajagopalan, N.; Lindenbaum, S. *Biochim. Biophys. Acta* **1982**, *711*, 66–74.
(9) Moore, E.; Celic, L.; Ostrow, J. D. *Gast.oenterology* **1982**, *83*, 1079–1089.
(10) Kahn, M. J.; Lakshminarayanajah, N.; Trotman, B. W.; Chun, P.; Kaplan, S. A.; Margulis, C. *Hepatology* **1982**, *2*, 732.
(11) Hofmann, A. F. *Hepatology* **1984**, *4*, 199S–208S.
(12) Schoenfield, L. J.; Lachin, J. M. *Ann. Intern. Med.* **1981**, *95*, 257–282.
(13) Nakagawa, S.; Makino, I.; Ishizaki, T.; Dohi, I. *Lancet* **1977**, *2*, 367–369.
(14) Bateson, M. C.; Bouchier, I. A. D.; Trash, D. B.; Maudgal, D. P.; Northfield, T. C. *Br. Med. J.* **1981**, *283*, 645–646.
(15) Gleeson, D.; Murphy, G. M.; Dowling, R. H. *Gastroenterology* **1985**, *88*, 1661.
(16) Dumont, M.; Erlinger, S.; Uchman, S. *Gastroenterology* **1980**, *79*, 82–89.
(17) Moore, E. *Hepatology* **1984**, *4*, 228S–243S.
(18) Gmelin, L. *Handbuch der Anorganischen Chemie*; Teil B, Lieferung 3; Verlag Chemie: Weinheim/Bergstr, 1961; pp 1398–1404.
(19) Moore, E.; Ostrow, J. D. *Gastroenterology* **1985**, *88*, 1679.
(20) Deranleau, D. A. *J. Am. Chem. Soc.* **1969**, *91*, 4044–4054.
(21) Lenkinski, R. E.; Elgavish, G. A.; Reuben, J. *J. Magn. Reson.* **1978**, *32*, 367–376.
(22) Darnall, D. W.; Birnbaum, E. R. *J. Biol. Chem.* **1970**, *245*, 6484–6488.
(23) Matthews, B. W.; Weaver, L. H. *Biochemistry* **1974**, *13*, 1719–1725.
(24) Sowadski, J.; Cornick, G.; Kretsinger, R. H. *J. Mol. Biol.* **1978**, *124*, 123–132.
(25) Reuben, J. In *Handbook on the Physics and Chemistry of Rare Earths*; Gshneider, K. A., Jr., Eyring, L., Eds.; North-Holland: Amsterdam, 1979; Vol. 4, Chapter 39, pp 515–552.
(26) Horrocks, W. DeW., Jr.; Sudnick, D. R. *J. Am. Chem. Soc.* **1979**, *101*, 334–340.
(27) Lee, L.; Sykes, B. D. *Biophys. J.* **1980**, *32*, 193–210.
(28) Reuben, J.; Elgavish, G. A. In *Handbook on the Physics and Chemistry of Rare Earths*; Gshneider, K. A., Jr., Eyring, L., Eds.; North-Holland: Amsterdam, 1979; Vol. 4, Chapter 38, pp 483–514.

the dissociation constants for taurocholate complexes are about 5 times higher than the corresponding ones for glycocholate, indicating a significantly stronger metal binding by the latter.

Experimental Section

Materials. Analytical grade chemicals are used throughout. Sodium glycocholate (Sigma Chemical Co, St. Louis, MO) is extracted at pH 5 in sodium phosphate buffer with ethyl acetate to remove cholic acid. The solution is acidified with HCl, and the precipitated glycocholic acid is washed with ice-cold water and dissolved in a minimum volume of ethanol, titrated with aqueous NaOH, and freeze dried. The sodium salt is redissolved in D_2O (Aldrich Chemical Co, Milwaukee, WI, 99.8% D), the pH adjusted to 9, and the sample lyophilized to remove residual H_2O.

Sodium taurocholate (Sigma) is solubilized in D_2O, lyophilized, and redissolved in D_2O. The bile salt solutions are freshly prepared from the lyophilized material and the concentrations determined by a 3α-hydroxysteroid dehydrogenase procedure.[29]

Dysprosium chloride (99.998%) is purchased from Aldrich. Stock solutions are prepared in D_2O, dried under vacuum by using a rotavapor (Buchi, Brinkmann Instruments, Westbury, NY) at 50 °C, and redissolved in D_2O. The concentration is determined by EDTA titration in 100 mM pyridine chloride buffer (pH 6), and arsenazo is used as the end-point indicator.

Methods

^{1}H NMR. Samples (0.5 mL) are prepared containing 0.5 mM sodium glycocholate or 1 mM sodium taurocholate. No buffer is used in any of our experiments. For the competition studies, $CaCl_2$ at 10 or 50 mM or NaCl at 150 or 300 mM is included in the solution. $DyCl_3$ is added in aliquots and the pH is adjusted to pH 5.0 unless otherwise indicated. Sodium 2,2-dimethyl-2-silapentane-5-sulfonate (DSS) at a final concentration of 0.1 or 0.2 mM is included in the sample as internal standard for chemical shift referencing. ^{1}H NMR spectra of the bile salt complexes are obtained at 400.1 MHz on a Bruker WH-400 spectrometer. Between 2000 and 8000 free induction decays are accumulated at 25 °C by using a 90° pulse width of 16 μs, spectral width of 4000 Hz, 4K memory, and line broadening of 1 Hz and are Fourier transformed to obtain each spectrum.

Analysis of the NMR Data. When conditions of fast exchange between the complexed and uncomplexed state prevail relative to the NMR time scale, the observed spectral position $\delta(i)$ of any resonance i is given by eq 1 where $\delta_M(i)$ is the intrinsic shift of

$$\delta(i) = \delta_M(i)[ML]/[L]_t \quad (1)$$

resonance i in the fully metal-bound position relative to the chemical shift position in its free state. [ML] and $[L]_t$ denote the equilibrium concentration of the metal-bound ligand and the total ligand concentration, respectively. The equilibrium concentration of the bound ligand is a function of the total concentration of ligand and metal ion as well as of the dissociation constants of the complexes formed. The gradual shift of the resonances from their original, unbound position as a function of Dy^{3+} added indicates a fast exchange of the individual glycocholate molecules between a metal-bound state and a free state on the time scale of the induced shifts. In the case of a 1:1 complex between Dy^{3+} and glycocholate, the complex is formed according to the equilibrium reaction where M and L are the free metal ion

$$M + L \rightleftharpoons ML \quad (2)$$

and free ligand, respectively, and ML is the metal ion–ligand complex. The apparent dissociation constant K_{app} (i.e., expressed in terms of concentration rather than activity) of the metal ion–ligand complex is given by eq 3 and the concentration of the complex can be expressed by the quadratic equation 4 where $[L]_t$

$$K_{app} = [M][L]/[ML] \quad (3)$$

$$[ML]^2 - ([M]_t + [L]_t + K)[ML] + [L]_t[M]_t = 0 \quad (4)$$

and $[M]_t$ are the total ligand and metal concentrations, respectively. By use of an iterative computer program, as shown on the flow chart in Figure 1, K and $\delta_M(i)$ are varied over wide ranges.

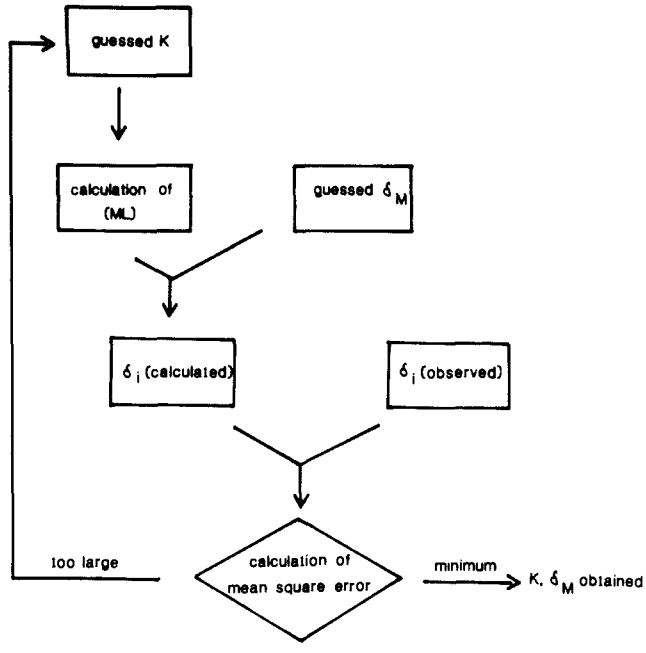

Figure 1. Flow chart for an iterative computer program to determine the dissociation constants (K) and intrinsic induced shifts (δ_M).

The values of $\delta(i)$ are then calculated by using eq 4 and 1. By comparison of these calculated values of $\delta(i)$ with the observed values, the mean-square error of the fit is calculated as the sum of the squares of the deviations divided by the number of data points. The experimental errors, which come from the inaccuracy in the determination of the chemical shift positions of resonances with large linewidths, are embedded in the mean-square errors. Final values for K and $\delta_M(i)$ are obtained when a sharp minimum of the mean square error of the fit is reached. Refinement of these values is carried out by substitution of eq 1 into eq 4 and its rearrangement as follows:

$$[M]_t = \delta(i)(\delta(i)[L]_t - \delta_M(i)([L]_t + K_{app}))/(\delta_M(i)(\delta(i) - \delta_M(i))) \quad (5)$$

Experimental data, $[M]_t$ and $\delta(i)$, are fitted to this equation by using the nonlinear program NLIN.[30] Both K and δ_M are calculated by using the Gly(α) ^{1}H data. The value of K is then substituted in eq 5, and the values of $\delta_M(i)$ are calculated for individual ^{1}H(i) resonances. The most accurate values for the simultaneous determination of both constants K and δ_M will be obtained when the saturation factor $s = [ML]/[L]_t$ lies between 0.2 and 0.8. For s values outside this range, the determined constants will become uncertain, and the expected error can be estimated by using the relative error computed by Deranleau (cf. Figure 1 in ref 20).

In each system, once K is determined, the equilibrium concentration of the complex can be calculated for every concentration of the components. When a competing metal ion is present, the same procedure is used to obtain $\delta_M(i)$ and the apparent dissociation constant (K') for the complex. The dissociation constant for the competing metal (K_I) is calculated by using eq 6 where [I] is the concentration of the competing metal ion.

$$K_I = [I]/(K'/K_{app} - 1) \quad (6)$$

In addition to the above procedures, an alternative method for calculating competition constants is also utilized. The binding equation can be rearranged to eq 7. By use of the calculated,

$$[ML] = [L]_t[M]_{free}/(K_{app} + [M]_{free}) \quad (7)$$

intrinsic induced shift, the equilibrium concentration of the complex is obtained from eq 1. The free Dy^{3+} concentration is calculated by subtracting the bound Dy^{3+} from the total. The

(29) Barnes, S.; Chitranukroh, A. *Ann. Clin. Biochem.* **1977**, *14*, 235–241.

(30) The NLIN program is part of the SAS package, SAS Inc., Cary, NC, 1980.

Table I. Intrinsic Dy-Induced Shifts[a,b] of ^1H Resonances of the Glycocholate (GC)–Dysprosium Complex

	$\delta_M(i)$, ppm				
proton(i)	control	10 mM Ca	50 mM Ca	150 mM Na	300 mM Na
Gly(α)	28.0 ± 0.20	26.30 ± 2.76	28.0 ± 0.62	28.70 ± 0.18	31.0 ± 0.06
H23(A)	3.50 ± 0.04	3.60 ± 0.03	3.60 ± 1.19	3.60 ± 0.03	3.50 ± 0.03
H23(B)	3.10 ± 0.02	3.30 ± 0.03	3.50 ± 0.7	3.10 ± 0.03	3.30 ± 0.04
H21	1.13 ± 0.02	1.13 ± 0.04	1.17 ± 0.03	1.10 ± 0.01	1.20 ± 0.01
H18	0.53 ± 0.02	0.56 ± 0.01	0.56 ± 0.02	0.52 ± 0.01	0.60 ± 0.01
H19	0.09 ± 0.01	0.14 ± 0.01	0.12 ± 0.01	0.0. ± 0.01	0.10 ± 0.01
H3	0.09 ± 0.01	0.11 ± 0.01	0.08 ± 0.03	0.08 ± 0.01	0.14 ± 0.01
H7	0.09 ± 0.03	0.11 ± 0.01	0.08 ± 0.03	0.09 ± 0.01	0.08 ± 0.01
H12	0.56 ± 0.01	0.57 ± 0.02	0.56 ± 0.01	0.54 ± 0.01	0.56 ± 0.01
H16	1.85 ± 0.04	*c*	*c*	*c*	*c*
% error[d]	5	15	30	12	17

[a] Relative to the chemical shift position of the uncomplexed species; mean ± SEM. [b] Downfield positive. [c] Unresolved resonance. [d] Expected % error due to limited saturation range.

binding equation can be expressed in a double-reciprocal form (eq 8 and 9). When $1/[ML]$ vs. $1/[M]_{free}$ is plotted, K_{app} is

$$1/[ML] = (1/[M]_{free})(K_{app}/[L]_t) + 1/[L]_t \quad (8)$$

$$[ML] = (\delta(i)/\delta_M(i))[L]_t \quad (9)$$

calculated from the slope, and $1/[L]_t$ represents the intercept on the vertical axis. In the presence of a competing metal ion such as Ca^{2+} or Na^+, the nature of competition can be ascertained from the nature of the double-reciprocal plots. The dissociation constant of the complex between the competitive metal ion and the bile salt is given by eq 6.

For unbiased estimates of the dissociation constants, computerized nonlinear regression analysis of the binding data from each experiment has been carried out by using the program COMP.[31]

A higher order model of the Dy^{3+}–bile salt complex (1:2) is also considered by using computational procedures described in ref 21. The Dy^{3+}-induced shift is a sum of two contributions

$$\delta = [ML]\delta_1/[L]_t + 2[ML_2]\delta_2/[L]_t \quad (10)$$

and the dissociation constants are defined as

$$K_1 = [M][L]/[ML]$$

$$K_2 = [ML][L]/[ML_2]$$

where δ_1, K_1 and δ_2, K_2 are the parameters of the 1:1 and 1:2 complexes, respectively. The free substrate concentration can be expressed in a cubic equation (eq 11). Similarly to the 1:1 model,

$$[L]^3 + (2[M]_t - [L]_t + K_2)[L]^2 + K_2([M]_t - [L]_t + K_1)[L] - K_1K_2[L]_t = 0 \quad (11)$$

sets of K_1 and K_2 are varied over wide ranges. Equation 11 can be solved by using the Newton–Raphson method and the equilibrium concentrations of the 1:1 and 1:2 species calculated. These are used with the rearranged form of eq 9

$$[ML]/([L]_t\delta) = 1/\delta_1 - (2[ML_2]/([L]_t\delta))(\delta_2/\delta_1) \quad (12)$$

and the limiting shifts for δ_1 and δ_2 are obtained. δ is then calculated by using eq 10 and compared with the observed values. The mean-square error is then calculated as described for the 1:1 model until a sharp minimum is obtained. Discrimination of the better model to fit the data has been done on the basis of goodness of fit, i.e., random variation and minimization of the residuals with respect to the Dy^{3+} concentration. The reliabilities of these parameters are judged on the basis of the following criteria:[21] For the accurate determination of these parameters, the saturation factor s_j (where $j = 1, 2$) of the complex should be within the range $s_j = 0.2$–0.8.

Results

Glycocholate Complexes. The ^1H NMR spectrum of 0.5 mM sodium glycocholate (see chemical structure in Figure 2) in D_2O at pH 7 is depicted in Figure 3a. There are at least 10 well-resolved ^1H resonances: the single proton geminal to each of the three hydroxys 3β, 7β, and 12β; the three methyl groups 18, 19, and 21; one proton from the ring methylene 16, the side-chain methylenes 23 (protons A and B), and the glycine α-methylene protons, Gly(α). Identification of the various ^1H resonances has been done according to assignments published previously.[32]

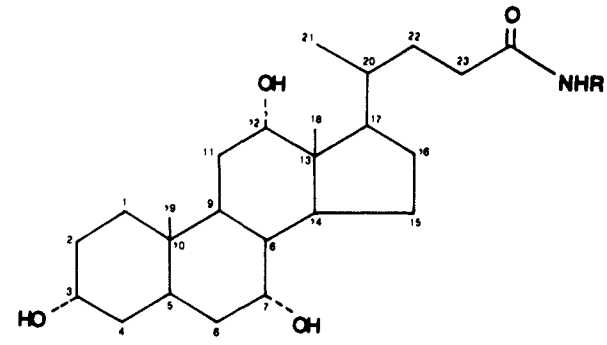

Figure 2. Chemical structure of conjugated cholic acids. Glycocholic acid: R = $CH_2{}^{\alpha}CO_2H$. Taurocholic acid: R = $CH_2{}^{\beta}CH_2{}^{\alpha}SO_3H$.

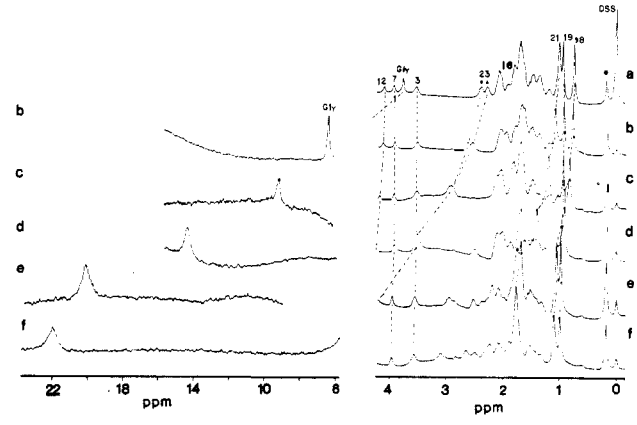

Figure 3. Effects of the addition of $DyCl_3$ on the ^1H spectra of sodium glycocholate (0.5 mM) in D_2O at pH* 5.0. The uppermost spectrum (a) is a control without added $DyCl_3$. The changes in chemical shift of individual ^1H resonances as $DyCl_3$ is added are marked with dotted lines (b–f). The concentration of $DyCl_3$ in b–f is 0.28, 0.68, 1.94, 3.57, and 4.44 mM, respectively. * is an impurity from D_2O.

Upon addition of increasing amounts of $DyCl_3$, while the sodium glycocholate concentration and the pH are kept constant, a gradually increasing downfield shift in the spectral position of most ^1H resonances is observed (Figure 3b–3f). The observed shift, δ, for each of the 10 resolved ^1H resonances is shown as a function of Dy^{3+} concentration in Figure 4. The intrinsic induced shifts are then calculated as described in the Methods section, and the results for a 1:1 complex are compiled in Table I. The magnitude of the shifts is in the order Gly(α) > H_{23} > H_{16} > H_{21} > H_{18} = H_{12} > H_{19} > H_3 = H_7. A dissociation constant of 4.15 ± 0.8 mM for the monomeric Dy^{3+}–GC complex has been obtained. The

(31) Cleland, W. W. In *Methods Enzymology*; Colowick, S. P., Kaplan, N. O., Eds.; Academic: New York, 1979; Vol. 63 Purich, D. L., Ed.), Chapter 6, pp 103–138.

(32) Barnes, S.; Geckle, J. M. *J. Lipid Res.* **1982**, *23*, 161–170.

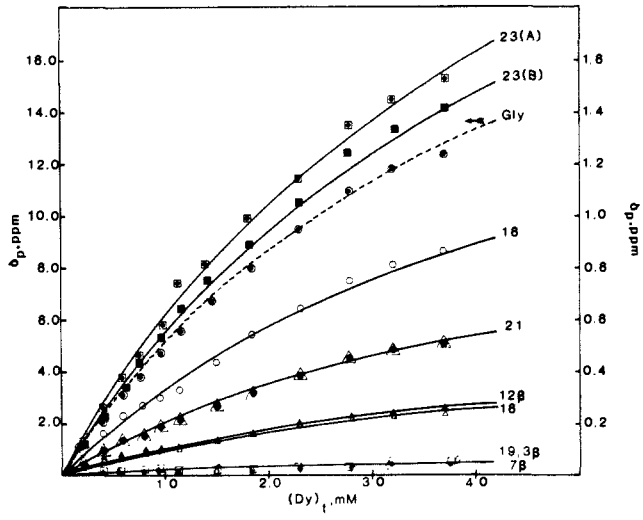

Figure 4. Relationship between added $DyCl_3$ and the induced chemical shift changes of individual ^1H resonances of glycocholate in dilute solution (0.5 mM) in D_2O at pH* 5.0. The symbols indicate experimental data, and the solid lines are the theoretical curves calculated for a 1:1 complex using the parameters in Tables I and II. Note that the scale for Gly(α) (left) is 10 times (0–18 ppm) larger than that for the other ^1H resonances (right) (0–1.8 ppm).

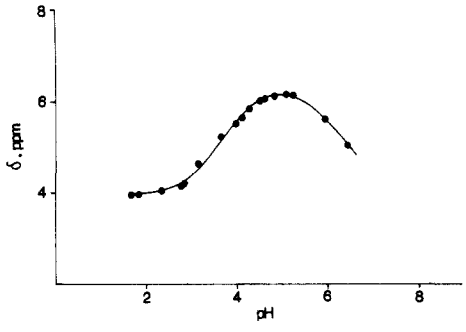

Figure 5. Effect of pH* on the chemical shift of the Gly(α) ^1H resonance of sodium glycocholate (0.5 mM) in D_2O induced by the addition of $DyCl_3$ (0.5 mM).

saturation factor varies between 0.02 and 0.43; therefore, K is determined with good accuracy, and the relative error is 5%.[20]

Attempts to fit the Dy^{3+}-dependent shift data with a model which includes 1:2 complexes produces unreasonably large intrinsic induced shifts, increases the total error sums of squares, and gives a systematic residual error. A sharp minimum of the mean-square error could not be obtained with any combination of K_1 and K_2. If the contribution of the 1:1 complex is much greater than that of the 1:2 complex, K_2 will be much larger than K_1 and the saturation factor s_2 will be $\ll 0.2$. Under these conditions, the 1:2 contribution is negligible and K_2 and δ_2 cannot be determined with good accuracy. In contrast, fitting the data to the 1:1 model results in random residual error, and a sharp minimum of the standard deviation is obtained. In monomeric solutions of glycocholate, therefore, dysprosium forms the cationic species, the so called "acid salt". By inference, this is probably the predominant species in calcium glycocholate as well.

The effect of pH on the magnitude of the Dy^{3+}-induced shift has been investigated since lanthanides form complexes with OH^- ions at neutral and basic pH, and because glycocholic acid has low aqueous solubility. The pH profile of the Dy^{3+}-induced shift is described by a bell-shaped curve with a maximum at pH 5.0 ± 0.2 (Figure 5). The Dy^{3+}-induced shift in the chemical shift falls to nearly zero at pH 2.0, indicating the removal of Dy^{3+} from glycocholate. The dissociation of Dy^{3+} from the glycocholate complex is most probably the result of protonation of the carboxylate function at low pH. Above pH 7, Dy^{3+} precipitates as the hydroxo complex and no Dy^{3+}-induced shift of the glycine α-methylene proton resonance is observed. Accordingly, further

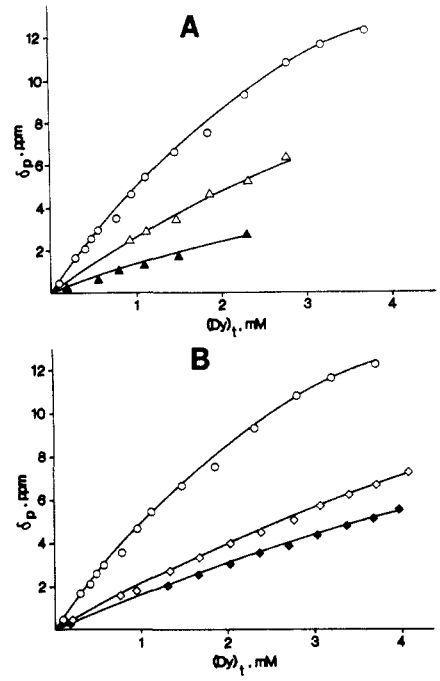

Figure 6. Modulation by $CaCl_2$ (A) and NaCl (B) of the dysprosium-induced chemical shift change of the Gly(α) ^1H resonance of 0.5 mM glycocholate in D_2O at pH* 5.0. The concentration of $CaCl_2$ was either 10 (△) or 50 mM (▲), whereas the concentration of NaCl was either 150 mM (◇) or 300 mM (◆). ○ is the control curve without added $CaCl_2$ or NaCl.

Table II. Dissociation Constants[a] of Metal–Bile Salt Complexes

metal ion	$K_{M\text{-}GC}$ (mM)	$K_{M\text{-}TC}$ (mM)	K_{TC}/K_{GC}
Dy^{3+}	4.15 ± 0.8 (0.2)[b]	25.2 ± 0.1 (1.01)[b]	6.1
Ca^{2+}	9.5 ± 1.4 (1.42)[b]	58.9 ± 0.2 (5.3)[b]	6.2
Na^+	92.1 ± 2.0 (14.7)[b]	178.0 ± 2.0 (14.2)[b]	1.9

[a] Mean ± SEM. [b] Expected error due to limited saturation range.

studies have been restricted to pH 5.0. It should be noted that the Ca^{2+}–glycocholate complex is soluble over a wider range of pH than Dy^{3+}–glycocholate. In any case, pH 5.0 is close to the physiologic pH in the upper small intestine.

When the Dy^{3+}-induced shift of the Gly(α) resonance is plotted against the Dy^{3+} concentration in the presence of Ca^{2+} or Na^+, there is a reduction in the Dy^{3+}-induced shifts of the glycocholate ^1H resonances as a function of added Ca^{2+} or Na^+ (Figure 6). The intrinsic induced shifts of the Dy^{3+}–glycocholate complex remain practically unaffected (Table I) within the limits of the saturation errors. Therefore, the observed induced chemical shifts can be used to calculate the concentration of the Dy^{3+}–glycocholate complex even in the presence of these competing metal ions.

This characteristic has been put to advantage in this study as can be seen in the double-reciprocal plots of the Dy^{3+} binding curves in the presence of 0, 10, and 50 mM $CaCl_2$ or 0, 150, and 300 mM NaCl. Each set of plots has the same intercept on the vertical axis (Figure 7), indicating that the number of binding sites is the same in each case. The value obtained is not significantly different from that of the glycocholate concentration (0.5 mM). The slopes of the plots, on the other hand, increase with increasing concentration of $CaCl_2$ or NaCl. These results indicate competition among Ca^{2+}, Na^+, and Dy^{3+} for the same binding site. Computerized nonlinear regression analysis has been used to obtain dissociation constants for the Dy^{3+}–glycocholate complex (4.15 ± 0.8 mM) and for the Ca^{2+} (9.6 ± 1.4 mM) and Na^+ (92.1 ± 2.0 mM) complexes. The same values for the dissociation constants have been obtained by using the iterative method (see Methods). The constants are compiled in Table II.

Taurocholate Complexes. The ^1H NMR spectrum of 1 mM sodium taurocholate in D_2O at pH 5.0 is similar to the glycocholate spectrum (Figure 3a), except for the taurine α- and β-methylene

Table III. Intrinsic Dy-Induced Shifts[a,b] of ^1H Resonances of Taurocholate (TC)–Dysprosium Complexes

	$\delta_M(i)$, ppm				
proton(i)	control	50 mM Ca	100 mM Ca	150 mM Na	300 mM Na
Tau(α)	−0.28 ± 0.01	−0.26 ± 0.01	−0.24 ± 0.01	−0.26 ± 0.01	−0.19 ± 0.01
Tau(β)	−0.52 ± 0.01	−0.52 ± 0.01	−0.51 ± 0.01	−0.53 ± 0.01	−0.48 ± 0.02
H23	0.68 ± 0.01	0.76 ± 0.02	0.74 ± 0.02	0.78 ± 0.08	0.84 ± 0.02
H21	0.09 ± 0.01	0.11 ± 0.01	0.11 ± 0.01	0.09 ± 0.01	0.16 ± 0.02
H18	0.11 ± 0.01	0.13 ± 0.01	0.12 ± 0.01	0.12 ± 0.01	0.13 ± 0.01
H19	0.17 ± 0.01	0.19 ± 0.01	0.18 ± 0.01	0.18 ± 0.01	0.19 ± 0.01
H3	0.16 ± 0.01	0.14 ± 0.01	0.17 ± 0.02	0.18 ± 0.01	0.16 ± 0.02
H7	0.15 ± 0.01	0.18 ± 0.01	0.19 ± 0.01	0.17 ± 0.01	0.18 ± 0.01
H12	0.14 ± 0.01	0.16 ± 0.01	0.16 ± 0.01	0.15 ± 0.01	0.17 ± 0.01
% error[c]	4	4	9	4	8

[a] Relative to the chemical shift position of the uncomplexed species; mean ± SEM. [b] Downfield positive. [c] Expected % error due to limited saturation range.

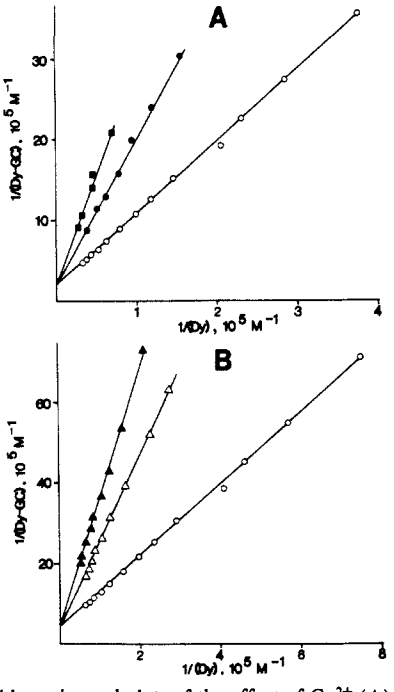

Figure 7. Double-reciprocal plots of the effect of Ca^{2+} (A) and Na^+ (B) on the dysprosium-induced chemical shift changes of the Gly(α) ^1H resonance of glycocholate (0.5 mM) in D_2O at pH* 5.0. The vertical axis is the reciprocal of the induced chemical shift change and the horizontal axis is the reciprocal of the free Dy^{3+} concentration. In A the concentration of $CaCl_2$ is 0 (○), 10 (●), or 50 mM (■). In B the concentration of NaCl is 0 (○), 150 (△), or 300 mM (▲).

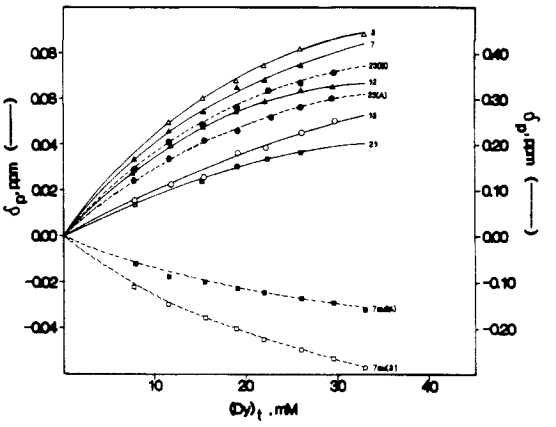

Figure 8. Relationship between added $DyCl_3$ and the induced chemical shift changes of individual ^1H resonances of a dilute (1.0 mM) solution of sodium taurocholate in D_2O at pH* 5.0. The scale for Tau(α), Tau(β), H_{23A}, and H_{23B} (right) is 5 times (−0.2–0.4) larger than that for the other resonances (left) (−0.04–0.08).

^1H resonances, Tau(α) and Tau(β). These appear at δ 3.5 and 3.06, respectively, and replace the Gly(α) resonance of 3.75 ppm. By the addition of increasing amounts of $DyCl_3$ to this solution, a gradually increasing upfield shift in the resonance positions of the Tau(α) and Tau(β) protons is observed, whereas all the other ^1H resonances shift downfield similarly to the glycocholate ^1H resonances (Figure 8). Analysis of the measurable induced shift data yielded the intrinsic induced shifts for some of the taurocholate ^1H resonances (Table III). The data conformed better to a 1:1 model rather than to one which includes a 1:2 complex, as was the case in the glycocholate system. The dissociation constant of this complex has been calculated to be 25.2 ± 0.11 mM (see Table II).

As in the case of glycocholate, addition of $CaCl_2$ or NaCl causes a reduction in the observed Dy^{3+}-induced shift without a significant effect on the intrinsic induced shift, thus permitting estimation of the bound and free Dy^{3+} concentrations. Double-reciprocal plots of the binding curves for Dy^{3+} to taurocholate in the presence of 0, 50, and 100 mM $CaCl_2$ and 0, 150, and 300 mM NaCl each intersect on the vertical axis, indicative of competitive inhibition (Figure 9). Computer analysis of these data using a nonlinear fitting procedure COMP,[31] as well as the iterative analysis as described in the flow chart in Figure 1, yield dissociation constants of 58.9 ± 0.17 and 178 ± 2.0 mM for the Ca^{2+} and Na^+ complexes, respectively (Table II).

Discussion

In the biliary and intestinal milieu, a fairly complex electrolyte system exists. The total concentrations of sodium and calcium metal ions, as well as that of the prevalent conjugated bile salts, glycocholate and taurocholate, and the pH are the major parameters determining the complex species formed. The role of calcium in forming physiologically important complexes of bile salts may be quite central.

Previously published dissocation constants of Ca^{2+}–taurocholate and Ca^{2+}–glycocholate complexes in dilute aqueous solution indicate a somewhat higher stability of the former relative to the latter.[9,17] This is surprising since the negatively charged group in glycocholate is a carboxylate, as opposed to the sulfonate group of taurocholate. One possible explanation could be additional, simultaneous interaction of the metal ion with one or more hydroxy groups of the cholanoate moiety. Such chelation would set some geometrical constraints on the bile salt ligand which might lead to a thermodynamical preference for bidentate binding in the case of the taurine system vs. that in the glycine system, due to the difference in side-chain flexibility. Another possibility could be that the particular dissociation constants were the result of the experimental method used, namely monitoring free Ca^{2+} concentration by a Ca^{2+}-specific electrode.

The use of the paramagnetic lanthanide, dysprosium, in the application of NMR to the study of Ca^{2+} and Na^+ binding to the glycine and taurine conjugates of cholate in dilute solution has satisfied the ideal requirements for the investigation of metal ion–bile salt interaction as set out in the Introduction. The results show that the metal ions Na^+, Ca^{2+}, and Dy^{3+} each have a greater affinity for glycocholate than for taurocholate. This is in contradistinction to two previous reports[9,17] in which the dissociation constant of the nonmicellar Ca^{2+}–taurocholate complex, deter-

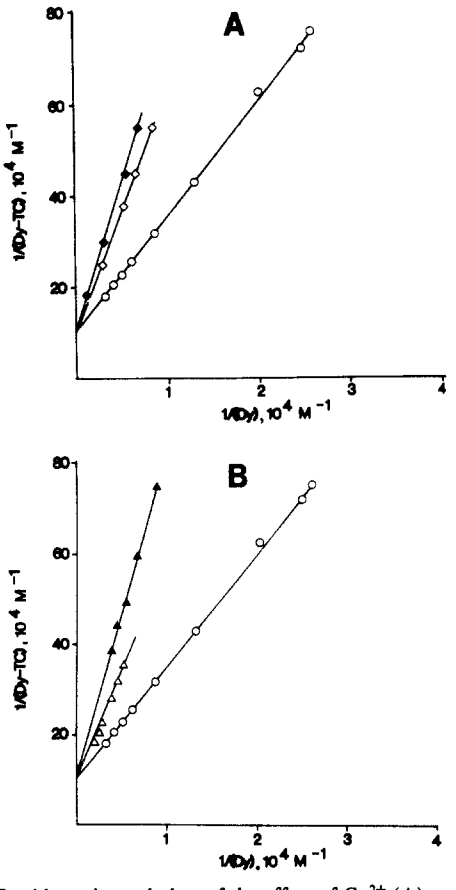

Figure 9. Double-reciprocal plots of the effect of Ca^{2+} (A) and Na^+ (B) on the induced chemical shift changes of the Tau(β) ^1H resonance of taurocholate (1 mM) in D_2O at pH* 5.0 induced by increasing additions of $DyCl_3$. In A the concentration of $CaCl_2$ is 0 (○), 50 (◇), and 100 mM (◆). In B the concentration of NaCl is 0 (○), 150 (△), and 300 mM (▲).

mined with a Ca^{2+}-specific electrode, ranged from 1.6 to 6.3 mM, as compared to 13.3 mM for the dissociation constant of the nonmicellar Ca^{2+}–glycocholate complex.[17] Although the latter value approximates the one determined in the present study by paramagnetic NMR (9.5 mM), the Ca^{2+}-specific electrode studies were performed at constant ionic strength (300 mM), i.e., with approximately 300 mM NaCl present. Since we have also shown in the present study that Na^+ competes for binding to the same site as the other metal ions, it would have the effect of increasing the apparent dissociation constants of the Ca^{2+}–bile salt complexes. In solutions containing 300 mM NaCl, the apparent dissociation constants based on the NMR data in the current study would have been 40.4 and 158.2 mM for the Ca^{2+}–glycocholate and Ca^{2+}–taurocholate complexes, respectively. On the other hand, correction of the previously published dissociation constants for these complexes[17] for the effect of Na^+ competition yields dissociation constants of 2.5 and 3.1 mM for Ca^{2+}–taurocholate and Ca^{2+}–glycocholate, respectively.

The discrepancies mentioned above between the data obtained in the present study and previously published data[9,17] may be due to the binding of Ca^{2+} to sites on the bile salt molecule other than the side chain, specifically the hydroxy groups. However, this is unlikely for several reasons.

First, the intrinsic induced shifts indicate an overwhelming proximity of the metal ion to the side chain. The geometrical dependence of the lanthanide-induced shifts is by no means simple, and an exact analysis entails separation of contact and dipolar contributions, as well as the determination of additional experimental parameters.[28] All this is beyond the scope of this work, and the elucidation of the three-dimensional solution structure of metal–glycocholate complexes will be the subject of a separate publication. Nevertheless, the very large systematic decrease in the intrinsic shift (see Tables I and III), while considering protons away from the carboxylate end of the bile salt, is sufficient to substantiate the conclusion that the Dy^{3+} ion is bound via the carboxylate group only, without involvement of the hydroxy groups. Ca^{2+} affects the Dy^{3+}-induced ^1H chemical shifts as a simple competitive inhibitor. It, therefore, replaces Dy^{3+} at the carboxylate or sulfonate binding sites. Also, the K_{TC}/K_{GC} ratio for Ca^{2+} is very similar to that for Dy^{3+}, further indicating isomorphous behavior of the two metals. In contrast, the ratio for Na^+ is significantly smaller, implying a non-side-chain component in binding, in particular in TC. Consequently, we can conclude that Ca^{2+}, as Dy^{3+}, binds exclusively to the carboxylate group. On the other hand, this does not preclude binding of calcium to hydroxy groups in an independent manner.

Second, the intrinsic Dy^{3+}-induced effect for each of the observable ^1H resonances is not affected by the presence of Ca^{2+}. This important result means that Ca^{2+} does not bind independently to another site. If Ca^{2+} were to bind to the hydroxy groups, the repulsive effect between the charged metal ions would alter the orientation of the side chain and the position of the Dy^{3+} ion. This would change the distances from the metal ion to the neighboring protons, as well as the angle between the radius vector from the metal ion to a given proton and the principal magnetic axis of the Dy^{3+} ion. The intrinsic induced effect is very sensitive to such changes since it falls according to the inverse third power of the distance. The range of the angular factor which also affects the intrinsic shift is between 2 and −1. Nonetheless, if Ca^{2+}, but not Dy^{3+}, were able to complex simultaneously both the ionized group on the side chain and one or more of the hydroxy groups, this would not be discernible by the NMR methods used in this work.

In addition to competition among metal ions for binding to the carboxylate or sulfonate groups, there is the possibility of competition by protons. In these studies we have carried out each experiment at pH 5, i.e., $[H^+] = 0.01$ mM. Since the pK_a of glycocholic acid has been reported as 3.8,[1] the corresponding proton dissociation constant is 0.16 mM. Therefore, the effect of competing protons on the dissociation constants of the various metal ion–glycocholate complexes at pH 5 should be minor, i.e., about 6%. Since the pK_a of taurocholic acid is approximately 1.56, it has a proton dissociation constant of 27.5 mM.[33] Thus, at pH 5.0 the effect of competition by protons (0.01 mM) on the metal ion–taurocholate dissociation constants is negligible. It is noteworthy that glycocholate displays a much greater affinity for proton binding than taurocholate. Metal ions compete with protons, and by corrollary the possibility exists that they may serve to somewhat reduce the pK_a of glycocholate, but not of taurocholate in the acidic intestinal milieu. Indeed, Figure 5 indicates a pK_a of 3.6 in the presence of a 1:1 Dy^{3+} complex of GC at 0.5 mM concentration.

Van der Meer and De Vries have recently shown that glycocholate binds to precipitated calcium phosphate to a greater extent than taurocholate.[34] This also supports the idea of a greater affinity of Ca^{2+} for glycocholate than for taurocholate. In addition, other investigators, using Ca^{2+}-specific electrodes, have shown that under micellar conditions Ca^{2+} binding to glycine-conjugated bile salts is tighter than to taurine-conjugated bile salts.[6,8,16]

It is also of interest that in dilute solutions the data are consistent with a 1:1 stoichiometry of the Ca^{2+}–bile salt complex, termed the acid salt by Moore et al.[9] The same stoichiometry is also reported in studies using the Ca^{2+}-specific electrode[9,17] and in crystals resulting from mixtures of saturated $CaCl_2$ and sodium cholate solutions.[35]

Our studies have not addressed metal ion binding in the dihydroxy bile salt systems. Other investigators, using Ca^{2+}-specific electrodes[8,16,19] or metallochromic dyes,[36] have found that the

(33) Ekwall, P.; Rosendahl, T.; Lofman, N. *Acta Chem. Scand.* **1957**, *11*, 590–598.
(34) Van der Meer, R.; De Vries, H. T. *Biochem. J.* **1985**, *229*, 265–268.
(35) Hogan, A.; Ealick, S. E.; Bugg, C. E.; Barnes, S. *J. Lipid Res.* **1984**, *25*, 791–798.
(36) Oehlberg, D. G.; Dubinsky, W.; Adcock. E. W.; Lester, R. *Am. J. Physiol.* **1984**, *247*, G112–G115.

apparent dissociation constants of Ca^{2+}–dihydroxy bile salt complexes are dependent on the position and orientation of the hydroxy groups. It is possible for these bile salts that particular structural configurations favor complexation of Ca^{2+} between ionized side chains and the hydroxy groups. On the other hand, the difference in Ca^{2+} binding to dihydroxy vs. trihydroxy bile salts may be influenced by factors such as weaker metal ion binding to micelles, the critical micellar concentration, and the solubility product of the bile salt–metal ion complex (Jones, C. A.; Hofmann, A. F.; Mysels, K. J.; Roda, A., unpublished data). Therefore, our conclusions about the absence of Ca^{2+} chelation to hydroxy groups for the trihydroxy bile salt systems are not necessarily transferable to the dihydroxy bile salts.

The biological implication of our data is that species which have a large excess of taurocholate will be less able to lower free Ca^{2+} activity than those with glycocholate. This may be a reason why dogs, which have mostly taurocholate in the bile, have evolved with a low cholesterol saturation index, whereas omnivores such as man and hamsters tolerate cholesterol supersaturation in the bile. The ratio of glycocholate to taurocholate in humans is about 3:1, and the concentration of total calcium in the bile is 3–5 mM. Since cholesterol gallstone formation in man requires other initiating factors besides a cholesterol supersaturated bile, such as a precipitated calcium nidus, the role of bile salts in suppressing the effects of free Ca^{2+}, in particular glycocholate, which has a calcium dissociation constant of 9.5 mM, may have had a major evolutionary influence on the physiology and chemistry of the biliary system.

Acknowledgment. This study was supported in part from funds derived from Grant AM-25511 from the National Institute of Arthritis, Metabolism, Digestive and Kidney Diseases and from funds for a pilot project from the Cystic Fibrosis Foundation. The NMR instrumentation used was supported in part by NIH Grant CA-13148 to the NMR Core Facility of the UAB Comprehensive Cancer Center. We thank Dr. Alan F. Hofmann, University of California, San Diego, for providing us, prior to publication, with a copy of his results.

Registry No. GC, 475-31-0; TC, 81-24-3; Ca, 7440-70-2; Na, 7440-23-5; Dy, 7429-91-6.

(37) Abbreviations: GC, 3α,7α,12α-trihydroxy-5β-cholan-24-oylglycine (glycocholate); TC, 3α,7α,12α-trihydroxy-5β-cholan-24-oyltaurine (taurocholate); NMR, nuclear magnetic resonance; EDTA, ethylenediaminetetraacetic acid; DSS, sodium 2,2-dimethyl-2-silapentane-5-sulfonate; pH*, uncorrected pH measured in D_2O; Gly, glycine; Tau, taurine.

Phototransformed Bleomycin Antibiotics. Structure and DNA Cleavage Activity†

Takashi Morii,‡ Teruo Matsuura,‡ Isao Saito,‡ Tadashi Suzuki,§ June Kuwahara,§ and Yukio Sugiura*§

Contribution from the Department of Synthetic Chemistry, Faculty of Engineering, and Faculty of Pharmaceutical Sciences, Kyoto University, Sakyo-ku, Kyoto 606, Japan.
Received March 27, 1986

Abstract: The light irradiation of copper(II)–bleomycin and its bithiazole model compound, methyl 2′-methyl-2,4′-bithiazole-4-carboxylate, induced isomerization of the 2,4′-bithiazole ring system to 4,4′-bithiazole. Phototransformed bleomycin and the model compound were isolated in high yields by using high-performance liquid chromatography. The electronic absorption, fluorescence emission, and ^1H and ^{13}C NMR data of the new photoproducts were compared with those of the original bleomycin and the model compound. Of special interest is the fact that the phototransformed bleomycin showed the nucleotide sequence cleavage mode to be essentially the same as that of the parent bleomycin. The present results provide valuable information not only for the photoreactivity of bleomycin antibiotics but also for the DNA recognition of the bithiazole group.

Bleomycin antibiotics have been clinically employed for the treatment of squamous cell carcinoma and malignant lymphoma. The oxidative DNA strand scission mediated by certain metallobleomycins is believed to be responsible for their therapeutic effects.[1] Usually, the DNA cleavage of bleomycin is thought to result from metal chelation and oxygen activation by the β-aminoalanine–pyrimidine–β-hydroxyhistidine moiety and DNA interaction by the bithiazole–terminal amine portion.[2] Recently, bleomycin antibiotics are reported to be photosensitive. We found that the bleomycin–Fe(III) complex produced prominent DNA strand scission by photoirradiation as well as by the presence of reductants or hydrogen peroxide.[3] By contrast, the bleomycin–Co(III) complex significantly degraded isolated DNA only by light irradiation.[4,5] While the UV irradiation of bleomycin alone by a medium-pressure mercury lamp or a xenon 300-W lamp induced the decrease of the absorption band at 290 nm due to the bithiazole chromophore,[6,7] details of the photoreaction of bleomycin antibiotics are entirely unknown. It is of particular importance to clarify the photolability of bleomycin in association with its DNA cleavage activity. Moreover, the role of the bithiazole group is still questionable in the bleomycin action on DNA.

Herein, we first demonstrate a transformation of the bithiazole group by light irradiation of the bleomycin–Cu(II) complex. Of interest is the fact that the nucleotide sequence cleavage mode of the phototransformed bleomycin was remarkably similar to that of the original bleomycin. The present results provide useful

† This paper is dedicated to Prof. Morio Ikehara for the occasion of his retirement from Osaka University in March, 1986.

‡ Faculty of Engineering.

§ Faculty of Pharmaceutical Sciences.

(1) Umezawa, H. In *Bleomycin: Current Status and New Developments*; Carter, S. K., Crooke, S. T., Umezawa, H., Eds.; Academic: New York, 1978; pp 15–19.

(2) Sugiura, Y.; Takita, T.; Umezawa, H. In *Metal Ions in Biological Systems*; Sigel, H., Ed.; Marcel Dekker: New York, 1985; Vol. 19, pp 81–108.

(3) Sugiura, Y.; Suzuki, T.; Kuwahara, T.; Tanaka, H. *Biochem. Biophys. Res. Commun.* **1982**, *105*, 1511–1518.

(4) Chang, C.-H.; Meares, C. F. *Biochemistry* **1984**, *23*, 2268–2274.

(5) Suzuki, T.; Kuwahara, J.; Goto, M.; Sugiura, Y. *Biochim. Biophys. Acta* **1985**, *824*, 330–335.

(6) Thakrar, N.; Douglas, K. T. *Cancer Lett. (Shannon, Irel.)* **1981**, *13*, 265–268.

(7) Antholine, W. E.; Sarna, T.; Sealy, R. C.; Kalyanaraman, B.; Shields, G. D.; Petering, D. H. *Photochem. Photobiol.* **1985**, *41*, 393–399.

0002-7863/86/1508-7089$01.50/0